The Journal of Experimental Biology 210, 4136-4149
Published by The Company of Biologists 2007
doi:10.1242/jeb.011197

Automatic aeroelastic devices in the wings of a steppe eagle *Aquila nipalensis*

Anna C. Carruthers, Adrian L. R. Thomas and Graham K. Taylor*
Department of Zoology, University of Oxford, Tinbergen Building, South Parks Road, Oxford, OX1 3PS, UK
*Author for correspondence (e-mail: graham.taylor@zoo.ox.ac.uk)

Accepted 11 September 2007

Summary

Here we analyse aeroelastic devices in the wings of a steppe eagle *Aquila nipalensis* during manoeuvres. Chaotic deflections of the upperwing coverts observed using video cameras carried by the bird (50 frames s^{-1}) indicate trailing-edge separation but attached flow near the leading edge during flapping and gust response, and completely stalled flows upon landing. The underwing coverts deflect automatically along the leading edge at high angle of attack. We use high-speed digital video (500 frames s^{-1}) to analyse these deflections in greater detail during perching sequences indoors and outdoors. Outdoor perching sequences usually follow a stereotyped three-phase sequence comprising a glide, pitch-up manoeuvre and deep stall. During deep stall, the spread-eagled bird has aerodynamics reminiscent of a cross-parachute. Deployment of the underwing coverts is closely phased with wing sweeping during the pitch-up manoeuvre, and is accompanied by alula protraction. Surprisingly, active alula protraction is preceded by passive peeling from its tip. Indoor flights follow a stereotyped flapping perching sequence, with deployment of the underwing coverts closely phased with alula protraction and the end of the downstroke. We propose that the underwing coverts operate as an automatic high-lift device, analogous to a Kruger flap. We suggest that the alula operates as a strake, promoting formation of a leading-edge vortex on the swept hand-wing when the arm-wing is completely stalled, and hypothesise that its active protraction is stimulated by its initial passive deflection. These aeroelastic devices appear to be used for flow control to enhance unsteady manoeuvres, and may also provide sensory feedback.

Supplementary material available online at
http://jeb.biologists.org/cgi/content/full/210/23/4136/DC1

Key words: bird flight, *Aquila nipalensis*, flight control, stability, aeroelastic device, high-lift device, flow control, leading-edge flap, Kruger flap, alula.

Introduction

The wings of birds are adapted to operate over an extraordinarily wide range of configurations, from the relatively rigid geometries of gliding to the highly flexible kinematics of flapping. This range is extended still further during take-off, landing and manoeuvring, when the wings must retain control authority while operating at high angles of attack and generating highly unsteady flows. All of this is achieved whilst operating in – and indeed exploiting – highly turbulent conditions. Here we ask how aeroelastic deflections of the covert feathers and alula enhance the range of wing configurations that birds are able to exploit.

Automatic aeroelastic wing deformation has been well documented for insects, which are obliged to make use of structural devices to effect changes in morphology because they lack muscles internal to their wings (e.g. Wootton, 1981; Ennos and Wootton, 1989; Wootton, 1993; Wootton et al., 1998; Wootton et al., 2000). Automatic aeroelastic wing deformation is much less well documented for birds, partly because previous work has focused on how changes in their kinematics are effected muscularly (e.g. Dial and Biewener, 1993; Tobalske and Dial, 1994). While muscles internal to the wings of birds undoubtedly drive most of their gross changes in morphology, aeroelastic deflection of, for example, the slotted tips of the primaries, can be extremely pronounced and is well known anecdotally (Graham, 1930; Withers, 1981; Azuma, 1992). Furthermore, high-speed film of barn swallows *Hirundo rustica* has been used to suggest an aerodynamic function for the tail streamers as automatic aeroelastic devices deflecting the leading edge of the tail (Norberg, 1994), and it therefore seems worthwhile to look for comparable aeroelastic devices in the wings of birds.

Anecdotal suggestions of an aeroelastic role for the covert feathers crop up occasionally in the engineering literature, including claims that covert feathers along the leading edge might operate in an analogous manner to the leading-edge flaps of high-performance aircraft (e.g. Hertel, 1963; Blick, 1976; Azuma, 1992), and that covert feathers on the upper surface of the wings might operate as turbulators or vortex generators (Blick, 1976; Stinton, 2001). Such suggestions have typically been made on the basis of isolated still photographs, and in this paper we aim to investigate the validity of these claims by providing a detailed analysis of the aeroelastic deflections of the covert feathers of a large bird of prey, the steppe eagle *Aquila nipalensis*, using onboard and high-speed digital video. While wind tunnel and laboratory experiments are suitable for

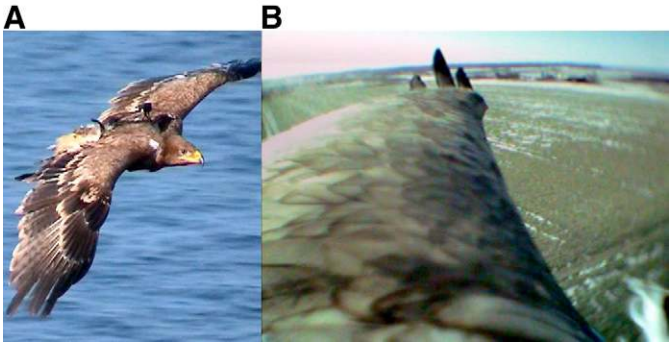

Fig. 1. (A) Photograph of steppe eagle carrying a wireless video camera while soaring freely over a sea cliff. (B) Still frame from the onboard video looking out along the left wing.

studying steady flight or short hops between perches (Pennycuick, 1968; Rosen et al., 2004), neither can explore the full extent of the flight envelope. Since pushing at the extremes of the flight envelope is likely to have driven much of the adaptive radiation in avian wing design, it is important that our understanding of bird flight should grow to encompass the full range of configurations utilised under natural conditions. Here we present an analysis of onboard video data collected using wireless cameras carried by a trained male steppe eagle during wide-ranging free flight in the field (Fig. 1), together with a more detailed analysis of indoor and outdoor perching manoeuvres, using high-resolution, high-speed digital video.

Few previous studies of bird flight have considered the function of the covert feathers (but see Brown and Fedde, 1993), despite the fact that these make up almost as large a proportion of the total wing surface area as the primaries, secondaries and tertials combined. The coverts provide all of the upper surface contour and most of the lower surface contour over the thick forward sections of the aerofoil. They are present throughout the anterior region in which leading-edge attachment and separation occur, and extend sufficiently far back to be influenced by trailing-edge separation. Fig. 2 shows the anatomical notation we use to describe both the underwing (Fig. 2A) and upperwing (Fig. 2B) coverts (after Brown et al., 1987). The primary coverts form the hand-wing contour, while the secondary coverts form the arm-wing contour. Among the secondary coverts, we distinguish between lesser, median and greater coverts, which form a series of rows progressing posteriorly from the leading edge. We use the aeroelastic deflections of these coverts to visualise the processes of flow attachment and separation that occur in free flight. This approach is analogous to the classical tuft-visualisation technique of wind tunnel engineering, which is useful for visualising qualitative features of surface flows (Barlow et al., 1999). The onboard video data are used to examine when each of the various passive aeroelastic phenomena we identify operates during wide-ranging natural free flight. The high-speed video data are then used to analyse the mechanics of covert feather deflection at higher spatial and temporal resolution for the specific case of perching.

We also use the same experimental methods as for the coverts to describe the aeroelastic deformation of the alula. The alula is widely recognised to operate as a high-lift device, although

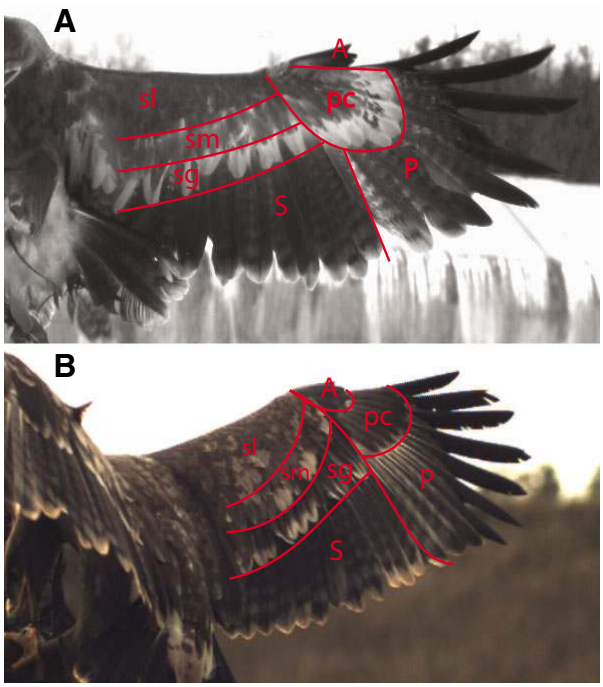

Fig. 2. Notation used to describe wing feathers of the upper (A) and lower (B) wing surfaces: A, alula; S, secondaries; P, primaries; sl, lesser secondary coverts; pc, primary coverts; sm, median secondary coverts; sg, greater secondary coverts. (After Brown et al., 1987.)

opinions differ as to whether it operates as a leading-edge slot/slat (e.g. Nachtigall and Kempf, 1971; Alvarez et al., 2001; Stinton, 2001; Meseguer et al., 2005) or a vortex generator (e.g. Videler et al., 2004; Videler, 2005). Because the alula feathers are muscularised at the base, the alula is usually assumed to operate as an active control device, although its potential for passive deflection has been noted on several occasions on the basis of wind tunnel studies on the wings of freshly killed birds (Graham, 1930; Brown, 1963; Nachtigall and Kempf, 1971). There appears to be no published detailed analysis of the kinematics of deployment of the alula in flying birds; we therefore use our observations of the aeroelastic deformation of the alula to clarify this aspect of its function. We conclude by discussing possible consequences of the aeroelastic phenomena we observe for sensory aspects of flight control and aerodynamic aspects of flow control.

Materials and methods

Animals

A captive 3-year old male steppe eagle *Aquila nipalensis* (Hodgson) of body mass 2.5 kg was used for all of the experiments, with an estimated chord Reynolds number $Re=2\times10^5$. This bird, called 'Cossack', had already been trained by its handler to carry miniature wireless video cameras and other equipment. The cameras and harness used in the study were less than 4% of the bird's total body mass and did not appear to interfere with the movements of the wings. Although this study samples only one individual, we have taken care to ensure that we have sampled it adequately, undertaking several days of testing in wide-ranging free flight using onboard video

cameras, and obtaining 37 independent high-speed video sequences of free-flight perching manoeuvres. We are therefore confident that the consistent feather deflections we describe are representative of the flight of the individual we used. We leave it to the reader to decide how far to extend our conclusions to other individuals of the same species, and indeed to other species of bird that have been anecdotally observed to use similar aeroelastic devices (Hertel, 1963; Blick, 1976; Azuma, 1992; Stinton, 2001).

The experimental protocol was approved by the United States Air Force, Surgeon General's Human and Animal Research Panel (SGHARP) for compliance with (i) Title 9 Code of Federal Regulations, *Animals and Animal Products*, chapter 1A, Animal Welfare, parts 1, 2 and 3; (ii) DOD Directive 3216.1, *Use of Laboratory Animals in DOD Programs*, 17 April 1995, as amended; (iii) AFMAN 40-401, *The Care and Use of Laboratory Animals in DOD Programs*, 1 December 2003 and (iv) *The Guide for the Care and Use of Laboratory Animals* – Institute of Laboratory Animal Resources, National Research Council, 1996. The experimental protocol was also evaluated by the Oxford University, Department of Zoology, Local Ethical Review Committee (LERC), and was considered not to pose any significant risk of causing pain, suffering, damage or lasting harm to the animal involved.

Experiments

Flight tests using onboard video cameras were conducted by releasing the eagle on a low sea cliff (Gjerrild Klint, Djursland, Denmark) over 3 days between 13 and 17 March 2006. During these tests, the eagle was allowed to soar freely up and down the ridge for several minutes at a time, which maximised the range of flight configurations and behaviours that were observed. Atmospheric conditions varied somewhat over the testing days, and are detailed below where relevant, but typical conditions were 0–3°C temperature and wind speeds between 3.5 and 9.5 m s^{-1} (TSI Hot Probe thermo-anemometer, TSI Inc., Shoreview, MN, USA).

Flight tests using high-speed digital video cameras were conducted under two experimental conditions, releasing the bird in either a large open field (Fuglslev, Djursland: 13–15 March 2006 and 18–23 October 2006; Abergavenny, Wales: 18–22 June 2007), or indoors in a 30 m long enclosed barn. In each case, the bird was encouraged to fly either to his handler's hand or to a wooden perch at which food was available. In total, we recorded 37 separate perching sequences, comprising 23 outdoor and 14 indoor sequences. Flying the bird in still air in a confined space indoors allowed us to elicit quite different flight behaviours during perching from those elicited outdoors, when the bird landed in a headwind of between 1.5 and 6.7 m s^{-1}. Specifically, whereas the eagle typically used a gliding approach outdoors, all indoor flights involved a flapping approach.

Onboard wireless video cameras

Two miniature wireless PAL video cameras (ZTV Model 809 2.4 GHz CMOS cameras, Inka Security Solutions Ltd, Farnborough, UK) were adapted for the bird to carry in flight (Fig. 1). The wireless cameras were mounted on the bird by means of a lightweight harness (total mass 66 g) custom-made from webbing material and Velcro™ straps in a rucksack-like arrangement with loose-fitting straps around the pectoral and pelvic girdle and longitudinal straps running dorsally and ventrally between them. The harness allowed the bird complete freedom of movement, but held the cameras relatively fixed, except during flapping when movements of the scapular region rocked the harness. The onboard cameras could be positioned dorsally or ventrally to allow coverage of the upper or lower surface of the wings.

The cameras were fitted with a pair of 90 mAh lithium polymer cells (LP90, Plantraco Inc., Saskatoon, Canada) giving up to 1 h of transmission time. The combined mass of each camera with batteries was <17 g, constituting <1% of body mass. The analogue video data were transmitted on different channels within the 2.4 GHz waveband and were received by two customised units (634-RX, Low Power Radio Solutions Ltd., Witney, UK) giving line-of-sight transmission with a range >200 m. The analogue video stream was recorded in DV format on MiniDV tapes by two digital camcorders (DCR-HC40E/HC42E Handycam, Sony Corporation, Tokyo, Japan) capable of receiving and converting an analogue video input. The onboard video data were downloaded in iMovie 3.0.3 (Apple Inc., CA, USA) and deinterlaced using JES Deinterlacer 2.7.4 (Jan E. Schotsman, 2004) to double the effective frame rate to 50 frames s^{-1}. This, of course, results in a drop in vertical image resolution, from 720×576 pixels to 720×288 pixels. Overall levels of image brightness and contrast were adjusted in Adobe Photoshop CS 8.0 (Adobe Systems Inc., 2003) for ease of viewing, but no further image processing was applied.

High-speed digital video camera

Additional data were collected using one or two tripod-mounted high-speed digital video cameras with internal batteries (2.6GB Redlake Motionscope M3, Lake Image Systems Ltd, Tring, UK). Video sequences were taken from a number of viewpoints to visualize both the upper and lower wing surfaces during various phases of perching in a series of flights between March 2006 and June 2007. The individual video sequences obtained are listed in Table 1, totalling 37 separate sequences. The cameras recorded up to 4096 monochrome 1024×1280 pixel images at 500 frames s^{-1} with a shutter time of 0.002 s, giving ca. 4 s of recording time. The cameras were post-triggered manually from a ruggedized laptop (Panasonic Toughbook CF51, Matsushita Electric Industrial Co. Ltd., Kadoma, Japan) running Redlake's MotionScope M3.0.0 software. Overall image levels of brightness and contrast were adjusted in Adobe Photoshop CS 8.0 (Adobe Systems Inc., 2003) for ease of viewing, but no further image processing was applied.

Results

Onboard video

Occurrence of covert feather deflection during flight manoeuvres

We observed 68 occurrences of deployment of the lesser underwing coverts using the onboard cameras, most of which occurred upon landing. We use the term 'deployment' to refer to any displacement of the feathers, without prejudice to whether it represents active elevation or passive deflection.

Since the lesser underwing coverts would frequently settle and redeploy several times during a single landing sequence, the number of recorded deployments corresponds to a smaller number of recorded landings. Mass deployment of the lesser underwing coverts was observed on all 24 of the landing sequences taken using the onboard cameras in which the lesser underwing coverts were visible. In addition, deployment of the lesser underwing coverts was observed on 33 (89%) of the 37 perching sequences taken using the high-speed cameras (Table 1). We therefore conclude that deployment of the lesser underwing coverts is a general and consistent feature of landing in the steppe eagle. Deployment of the lesser underwing coverts was also observed in all six of the flapping take-off sequences in which the underwing coverts were visible. Deployment always occurred during the downstroke on flapping take-offs, but in the majority of cases the position of the wings during take-off prevented us from seeing whether the lesser underwing coverts were deployed. Deployment of the lesser underwing coverts was also observed during five single wingbeats that interrupted soaring flight (Fig. 3). In addition to these deployments in landing manoeuvres and flapping, we observed two instances of underwing covert deployment during two separate bouts of soaring as the bird flew low over the cliff edge, which must have been associated with a significant updraft given the strong onshore breeze (Fig. 4).

Deployment of the underwing coverts was usually accompanied by deflection of the upperwing coverts and protraction of the alula. The alula is only visible in onboard video viewing the lower wing surface. Within this subsample of the data, protraction of the alula was observed within 100 ms of underwing covert deployment on 44 (81%) of the 54 occasions on which the underwing coverts were deployed. Occurrences of upper surface feather deflections are only visible in onboard video viewing the upper wing surface. Within this subsample of the data, upperwing covert deflections were observed at some

Table 1. *Summary of tests with high-speed video cameras*

Run	Experimental setup	Type of approach	Underwing coverts	Notes
1	Outdoor	Flapping	Deploy	
2	Outdoor	Gliding	Deploy	
3	Outdoor	Flapping	Deploy	
4	Outdoor	Gliding	Deploy	
5	Outdoor	Gliding	Deploy	Small wingbeat before landing
6	Outdoor	Gliding	Deploy	
7	Outdoor	Gliding	Partially deploy	Missed perch
8	Outdoor	Gliding	Deploy	
9	Outdoor	Gliding	Deploy	
10	Outdoor	Gliding	Not visible	
11	Outdoor	Gliding	Not visible	
12	Outdoor	Gliding	Not visible	
13	Outdoor	Gliding	Deploy	
14	Outdoor	Flapping	Deploy	
15	Outdoor	Gliding	Partially deploy	Touchdown manoeuvre with small wingbeat
16	Outdoor	Gliding	Deploy	
17	Outdoor	Gliding	Deploy	
18	Outdoor	Gliding	Partially deploy	
19	Indoor	Flapping	Deploy	
20	Indoor	Flapping	Deploy	
21	Indoor	Flapping	Deploy	
22	Indoor	Flapping	Deploy	
23	Indoor	Flapping	Deploy	
24	Indoor	Flapping	Deploy	
25	Indoor	Flapping	Deploy	
26	Indoor	Flapping	Deploy	
27	Outdoor	Gliding	Deploy	
28	Outdoor	Gliding	Deploy	
29	Outdoor	Gliding	Deploy	
30	Outdoor	Gliding	Deploy	
31	Indoor	Flapping	Partially deploy	Touchdown manoeuvre
32	Indoor	Flapping	Deploy	
33	Indoor	Flapping	Deploy	
34	Indoor	Flapping	Deploy	
35	Indoor	Flapping	Deploy	
36	Indoor	Flapping	Deploy	
37	Outdoor	Gliding	Don’t deploy	Touchdown manoeuvre

‘Flap’ refers to leading edge covert feathers.

point on all 14 occasions on which the underwing coverts were deployed. Deflections of the upperwing coverts do not exhibit the coherence of those on the lower wing surface, instead forming an interrupted and unstructured surface that can, however, affect most of the coverts. All six of the landing manoeuvres we observed from an onboard camera viewing the upper wing surface were associated with deflection of the upperwing coverts across the entire wing, indicative of flow separation over the entire suction surface of the wing. In contrast, the two gust-response manoeuvres (Fig. 4) and five flapping flight sequences (Fig. 3) we observed caused deflection of only the greater upperwing coverts, indicating that the flow was only separated at the trailing edge.

High-speed video

Occurrence of covert feather deflection during perching manoeuvres

Deflection of the covert feathers is very fast: the onboard video shows that the lesser underwing coverts typically transition from being fully settled to fully deployed within 60 ms. Since the temporal resolution of the onboard video (20 ms) is too coarse to resolve the details of events occurring in this short a timescale, we describe the detailed processes of covert feather deflection associated with perching sequences recorded using the high-speed video cameras. A total of 37 landing sequences were recorded using the high-speed cameras indoors or outdoors (Table 1) and deployment of the lesser underwing coverts was observed on 33 (97%) of the 34 sequences on which the feathers were visible. The only one of these 34 landing sequences on which the lesser underwing coverts did not deploy was a touchdown manoeuvre in which the eagle took food from his handler's hand without actually landing (Table 1, run 37).

Of the 37 landing sequences, 23 were filmed outdoors, comprising 20 gliding approaches (e.g. Fig. 5) and three flapping approaches (e.g. Fig. 6). Of these 20 gliding sequences, two ended in touchdown manoeuvres in which the bird took food from its handler's hand without actually perching. The remaining 14 landing sequences were filmed indoors and all involved flapping approaches, of which one ended in a touchdown manoeuvre (Table 1, run 31). Outdoors, the eagle made use of approximately 50–100 m for its gliding approaches. Indoors, the eagle had only 30 m available for its landing approach, which probably explains why only flapping approaches were observed. The absence of a headwind during indoor testing would also have contributed towards this tendency to flap on approach, although gliding approaches were observed outdoors in headwinds as low as 1.5 m s^{-1}. During outdoor testing, the bird always landed into the wind, and as its right wing would have been subject to interference from the handler's wake, we analyse outdoor high-speed video data for the left wing only. Results for the indoor high-speed video are also based on data for one wing only.

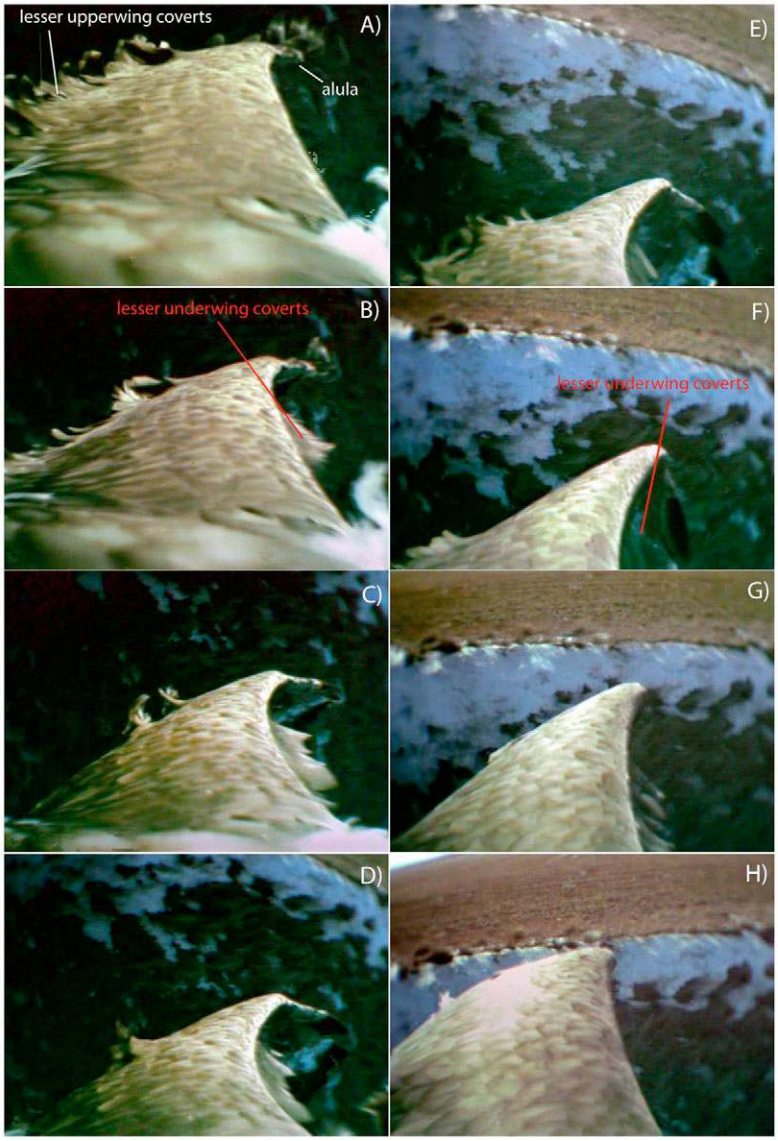

Fig. 3. Deflection of lesser upper- and underwing coverts during flapping flight over a sea cliff, showing the downstroke (A–D) and upstroke (E–H). Interval between images: 20 ms. An animation of this sequence is provided in supplementary material Movie 3.

Mechanism of covert feather deflection during gliding perching sequences

A typical gliding perching sequence involves three sequential phases: a gliding approach, a rapid pitch-up manoeuvre, and a deep stall. Deployment of the lesser underwing coverts usually occurs towards the end of the pitch-up manoeuvre and into the deep stall. Fig. 5 illustrates the three phases of a typical gliding perching sequence. The approach phase of a gliding perching sequence usually involves a glide close to the ground with the wing held fixed in a fully outstretched posture (Fig. 5A). The approach ends with the bird well below the height of the handler's arm, and as the distance between the wing and the ground is on the order of half its span at this point, the bird will be experiencing significant ground effect. During the gliding approach, the wing is held at a relatively low geometric angle

of attack, but reduction of the induced incidence by ground effect (Thwaites, 1960) will lead to a slightly higher effective angle of attack than would be the case if the bird were gliding at the same geometric angle of attack far from the ground.

As the eagle approaches its handler, it executes a rapid pitch-up manoeuvre (Fig. 5B–D) near to the ground. The nose-up pitching moment appears to be caused by a combination of the wings flexing (which brings the wrist and presumably the centre of pressure forward) and the tail tilting tip-up (which means that the tail presumably takes a less positive, or even negative, downwards, load). Simultaneously, the legs are swung forward in preparation for perching. The point of maximum wing flexion is sufficiently well defined to provide a convenient reference time t=0 ms (t_0; Fig. 5D) for comparing the timing of events between different sequences. At time t_0, the arm-wing and hand-wing are swept back through approximately 45° to give an overall M-shaped wing of comparatively low aspect ratio and area. This is the phase of the perching sequence during which the underwing covert feathers are deployed. The upperwing covert feathers also begin to deflect towards the end of the pitch-up phase, albeit less consistently, and not in such an obviously structured pattern.

Deployment of the lesser underwing coverts begins shortly before or after t_0 (Fig. 5E). For example, in the perching sequence illustrated in Fig. 5 there is no deployment visible at t=0 ms (Fig. 5D). At this point, the hand-wing is maximally swept and the leading edge of the arm-wing is highly curved. Typically, the anterior row of coverts deploys shortly after the point of maximum sweep, in a wave travelling from the wrist to the scapulars. In the sequence shown in Fig. 5, the wing has begun to straighten by t=40 ms (Fig. 5E) and a block of feathers is visibly deployed along the straight distal portion of the leading edge. By t=60 ms (Fig. 5F) the wing has straightened further and the coverts are deployed further inboard with a greater number of feathers recruited from the posterior as well as anterior rows. By t=80 ms (Fig. 5G,H) the feathers are fully deployed all along the straight leading edge.

Fig. 4. Deflection of lesser upper- and underwing coverts during a mid-flight gust response over a sea cliff. (A–D) Covert feather deployment and (E–H) covert feather retraction. Interval between images: 20 ms between rows; 320 ms between columns. The coverts remain in approximately the same deflected position between frames D and E. An animation of the complete sequence is provided in supplementary material Movie 4.

Table 2 gives the times of first deployment and full deployment of the underwing coverts from those five perching sequences in which they were visible throughout. First deployment was defined as the time at which the first covert feather was visibly deflected from the surface of the wing. Full deployment was defined as the first time at which the coverts were deflected along the entire length of the leading edge, regardless of the number of rows involved. The timings of first and full deployment were in the range t=–6 to 38 ms and t=48 to 100 ms, respectively, and are therefore consistent to within 52 ms between sequences. The interval between them varies between 48 and 80 ms, so is consistent to within 32 ms across the sequences (Table 2). Examination of the individual feathers at three points along the wing in each sequence suggests that while the complete row of lesser underwing coverts deploys within ca. 60 ms, the individual covert feathers take anything between 8 and 48 ms to deploy.

The time interval over which the complete row of lesser underwing coverts remains deployed is rather variable, ranging between 2 and 392 ms in the six perching sequences in which they were visible throughout (Table 2). Closure of the lesser underwing coverts usually occurs when the wings are fully extended and seems to be initiated either by nose-down rotation of the wing, corresponding to a reduction in the angle of attack, or elevation of the wing, as occurs at the beginning of an upstroke. The time taken for the complete row of lesser underwing covert feathers to close fully is also variable, ranging between 62 and 140 ms (Table 2), and whereas the coverts deploy in a travelling wave, they typically

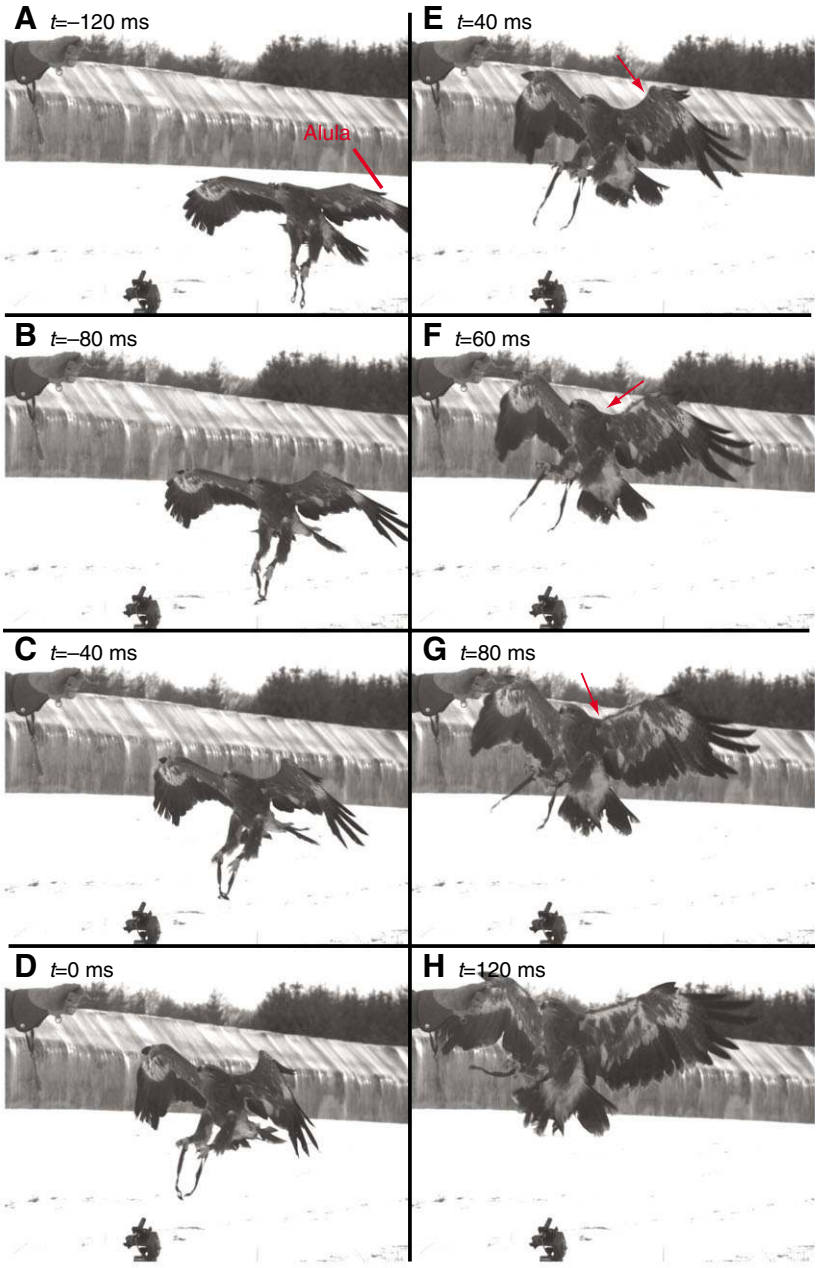

Fig. 5. Gliding perching sequence (Run 9 of Table 1) taken using high-speed digital video camera. Time of frame *t* is shown at upper left of each panel, referenced to the point of maximum wing flexion *t*=0 ms (D). Phase 1 (A): gliding approach. Alula begins to peel upwards; tail flicked up and back. Phase 2 (B–D): pitch-up manoeuvre. Wrist sweeps forward. (E) Lesser underwing coverts begin to deflect from wrist (red arrow); alula starts to protract; wing begins to straighten; tail spreads and pushes downwards and forwards. (F) Lesser underwing coverts deflecting in travelling wave from wrist towards shoulder (red arrow). (G) Lesser underwing coverts fully deflected (red arrow). Phase 3 (H): deep stall. Wings outstretched to give parachute-like shape. An animation of the complete sequence at 500 frames s^{-1} is provided in supplementary material Movie 5.

close as a single unit. Closure times of individual feathers, examined at three points along the wings in each of the three sequences, vary between 8 and 54 ms.

Even before the underwing coverts have first begun to deflect, the alula can be seen to peel up from the wing surface. This peeling starts at the tip (Fig. 7B), indicating that the alula is lifted passively from the wing surface in the initial stages of deployment. Although this shows definitively that the initial work of lifting the alula is being done aerodynamically, we cannot exclude the possibility that this peeling is initiated by a slight muscular deflection of the alula to modify the flow appropriately to then lift it passively. Nevertheless, in the five perching sequences in which the alula was clearly visible, active protraction of the alula from its base could only be seen after passive peeling from the tip had occurred (Fig. 7D). Initial peeling of the alula occurs well before t_0, in the range *t*=–222 to –102 ms (Table 2), and therefore well before deployment of the underwing coverts. Active protraction of the alula is first seen at around the same time as the underwing coverts begin to

Table 2. *Timing of lesser underwing covert feather deflection in gliding perching sequences*

Event	Time of occurrence (ms)				
Run	4	6	8	9	13
Alula begins to peel	–154	–222	–102	?	?
Hand-wing begins to sweep	–138	–90	–64	–122	?
Alula begins to protract	4	28	2	8	–34
Lesser underwing covert deployment					
Begins	–6	4	–4	38	20
Complete	56	64	48	92	100
Lesser underwing covert closure					
Begins	178	88	366	222	102
Complete	318	150	492	316	200

Times are referenced to the point of maximum wing flexion (t_0) and are accurate to ±4 ms.

deploy (Fig. 7D; Fig. 5E), in the range t=–34 to 28 ms (Table 2). Forward protraction of the alula therefore coincides with the point of maximum hand sweep. In summary, deployment of the alula is a two-stage process. Whereas the initial peeling of the alula occurs more or less normal to the wing surface, the active protraction of the alula sweeps it through approximately 45° forward from the leading edge.

Towards the end of the pitch-up manoeuvre, the wings re-extend in preparation for the final phase of perching: the deep stall. In this final phase, the tail is tilted tip-down and the wings are extended fully in a spread-eagled posture (Fig. 5H,I; Fig. 8). The angle of attack of the wings at this stage of the manoeuvre is close to 90°. At this point in the perching sequence, the upperwing secondary coverts exhibit massive deflection (Fig. 8C), indicative of flow separation over the entire suction surface of the arm-wing. Deflection of the upperwing primary coverts only ever occurs towards the very end of the deep stall phase, once the secondary coverts are already deflected. The wings and tail are therefore functioning more like a parachute than a conventional wing during the deep stall phase of perching (Fig. 9).

Mechanism of covert feather deflection during flapping perching sequences

A typical flapping perching sequence involves a flapping approach, followed by a single wingbeat with distinct kinematics, sometimes followed by a further wingbeat of low amplitude. Analogous to the second and third phases of a gliding perching sequence, the distinctive final or penultimate wingbeat of each sequence incorporates a rapid pitch-up manoeuvre leading to a deep stall, and appears to be the main source of deceleration. Deployment of the lesser underwing coverts occurred towards the end of each downstroke, and was observed on all 29 wingbeats recorded during 17 separate flapping sequences. Fig. 6 illustrates a typical flapping perching sequence.

During the flapping approach, the bird flies in at approximately the height of the perch and decelerates somewhat while producing sufficient lift to maintain level flight (Fig. 6A–D). The stroke plane is inclined sharply downwards during the flapping approach, and the tail beats forwards and downwards in phase with the wings, fanning out as it does so. The lesser underwing coverts consistently deploy towards the end of each downstroke (e.g. Fig. 6I; Table 3) and close at

Fig. 6. Flapping perching sequence (Run 14 of Table 1) taken using high-speed digital video camera. Time interval between frames: 40 ms. (A–D) final wingbeat of flapping approach. (E–L) Main deceleration wingbeat, involving pitch-up motion of wings (E–H) followed by deep stall (H–J). The lesser underwing coverts deploy towards the end of each downstroke and close shortly after the beginning of each upstroke (red arrows). An animation of the complete sequence at 500 frames s^{-1} is provided in supplementary material Movie 6.

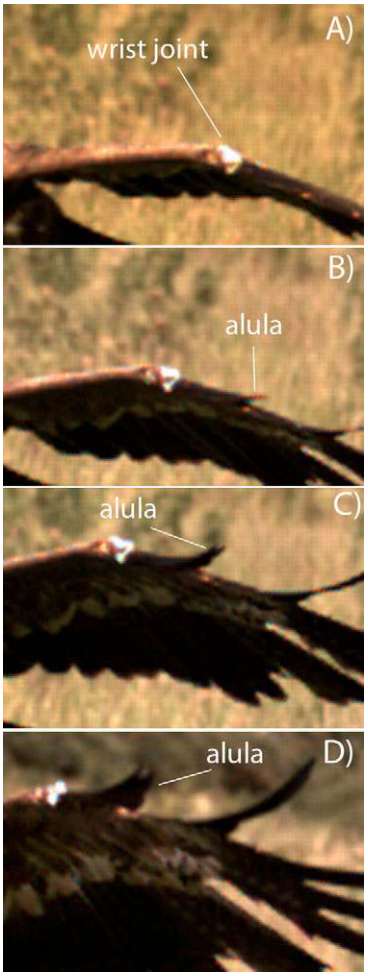

Fig. 7. Alula mechanics during gliding perching manoeuvre. Time interval between frames: 80 ms. (A) Alula is flush with the wing during the early stages of the gliding approach. (B) Alula peels from the tip towards the end of the gliding approach. (C) Hand-wing begins to sweep back, causing peeling alula to protrude further from wing surface. (D) Alula actively protracts. An animation of the complete sequence at 500 frames s^{-1} showing the entire bird is provided in supplementary material Movie 7.

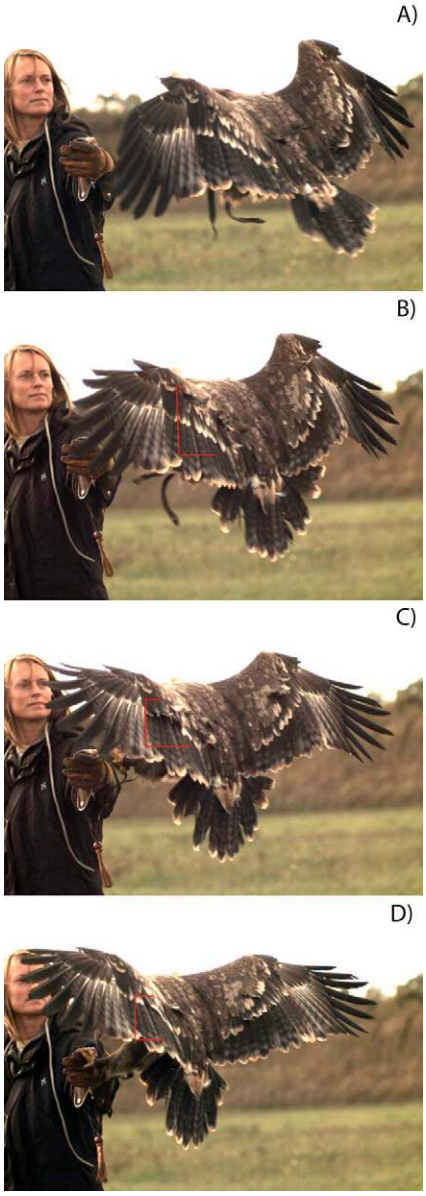

Fig. 8. Pitch-up phase of gliding perching sequence (A), leading into deep stall (B–D). Time interval between frames: 40 ms. Red brackets show extent of deflection of the secondary upperwing coverts. An animation of the complete sequence at 500 frames s^{-1} is provided in supplementary material Movie 8.

the beginning of the upstroke (e.g. Fig. 6C; Table 3). Active protraction of the alula occurs as the lesser underwing coverts begin to deflect, but the angle of the camera was such that we were unable to determine whether the alula began to peel passively before deployment of the underwing coverts, as was observed in gliding perching sequences.

Following the slowly decelerating flapping approach, the eagle makes a single wingbeat with distinctive kinematics, corresponding to the main deceleration phase of the flapping perching sequence. The stroke plane during this wingbeat is approximately horizontal, rather than inclined downward as on the wingbeats of the flapping approach. Analogous to the second phase of a gliding perching sequence, this main deceleration wingbeat ends in a rapid pitch-up motion of the wings. The legs are swung forwards in preparation for landing as the wings begin their downstroke (Fig. 6E) and the wings are pitched up with respect to the body (Fig. 6E–H), increasing their geometric angle of attack to approximately 90° to the horizontal, analogous to the third, deep-stall phase of a gliding perching sequence (Fig. 6H–J). At the same time, the tail is brought forward and fanned out to such an extent that the gap between tail edge and wings is closed, providing a continuous parachute-like surface that will maximise aerodynamic drag during the deep stall. Interestingly, the hand sweep that was observed during the pitch-up phase of gliding perching sequences is not observed during the pitch-up phase of flapping perching sequences, in which instead the arm section remains relatively straight throughout. As in the preceding wingbeats of the flapping approach, the lesser underwing covert feathers deploy

towards the end of the downstroke of the main deceleration wingbeat, and the alula protracts at about the same time (Fig. 6G–H; Table 3). Interestingly, the underwing coverts deploy as a single section, rather than as a wave travelling from wrist to shoulder, as was observed during gliding perching sequences.

The main deceleration wingbeat was followed by a further low-amplitude wingbeat in 8 of the 16 sequences for which the end of the landing was recorded on the video. The kinematics of this wingbeat are similar to those of the flapping approach phase preceding the main deceleration wingbeat, and the lesser underwing coverts deploy and close at similar times (Table 3). This wingbeat seemed to be used to fine-tune the final stage of the landing as necessary, which probably explains why it was not observed on all sequences.

The qualitative differences we observe between the kinematics of the main deceleration wingbeat and the wingbeats that precede or follow it are manifested in quantitative differences in the timing of deployment and closure of the lesser underwing coverts. We take the end of each downstroke as our reference time t_0 for comparing the timing of covert feather deployment on different wingbeats between and within sequences. We define the end of the downstroke by the movement of the primary feathers, since these are always visible, but note that upward recovery of the wrist joint is visible in some sequences before the primaries begin their upstroke. The timing of first deployment of the underwing coverts relative to the end of the downstroke differed significantly between the flapping approach wingbeats, main deceleration wingbeat and fine-tuning wingbeat (one-way ANOVA: P=0.01, $F_{2,20}$=5.99), as did the timing of the end of closure (one-way ANOVA: P=0.01, $F_{2,25}$=5.12). *Post hoc* comparisons of means (Tukey–Kramer honestly significant differences; α<0.05) showed that the timing of the start of deployment and the end of closure of the coverts occurred significantly later in the main deceleration wingbeat than in the wingbeats that preceded or followed it, but that there were no significant differences in the timing of covert deployment and closure between the flapping approach wingbeats and fine-tuning wingbeat. Although the coverts deployed and closed significantly later during the main deceleration wingbeat, the interval between deployment and closure did not differ significantly between wingbeats (one-way ANOVA: P=0.26, $F_{2,19}$=1.46). Protraction of the alula on each wingbeat began between 15 ms before and 26 ms after deployment of the lesser underwing coverts. This is comparable to the timing of protraction of the alula on gliding approaches (Table 2), which occurred between 34 ms before and 28 ms after deployment of the coverts. There is therefore a strong consistency in the timing of alula protraction across flapping and gliding perching sequences.

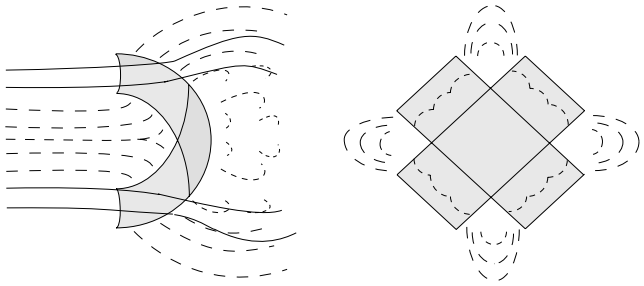

Fig. 9. Cartoon of cross-parachute aerodynamics. Broken streamlines denote jets passing between arms of parachute; solid streamlines denote flow that attaches and then separates from the upper surface. (Redrawn from Shen and Cockrell, 1988.)

Discussion

Patterns of flow separation in perching and other manoeuvres

Covert feathers are highly flexible structures, and although birds are able to erect their coverts during preening, for example, the muscles acting on them can only apply forces at the base of the feather. It is clear from our video sequences, however, that when the feathers are lifted away from the surface they rise first at the tip, which implies that their elevation represents a passive response. Although passive deflection could in principle occur as an inertial reaction to acceleration of the wings during flapping or morphing, the timing of the deflection of the feathers in relation to the acceleration of the wings is not consistent with this interpretation. We therefore conclude that the deflection of the coverts is a passive aeroelastic response: the feathers are rising because air flows under them – at least at the tips.

The deflections of the upperwing covert feathers therefore allow us to make certain inferences about the pattern of flow

Table 3. *Timing of lesser underwing covert feather deflection in flapping perching sequences*

	Flapping approach wingbeats			Main deceleration wingbeat			Fine-tuning wingbeat		
	N	*t* (ms)	s.d.	*N*	*t* (ms)	s.d.	*N*	*t* (ms)	s.d.
Alula begins to protract	1	–84	–	9	–82	46	4	–102	32
Time taken for alula to protract	1	24	–	8	26	13	4	29	18
Lesser underwing covert deployment									
Begins	3	–84	2	12	–62	13	8	–93	31
Complete	5	–23	33	12	–5	33	8	–44	34
Lesser underwing covert closure									
Begins	7	48	30	12	104	37	8	28	55
Ends	7	93	34.6	13	178	62	8	130	67

Values given are means with s.d., where applicable.
Times are referenced to the point of maximum wing flexion (t_0) and are accurate to ±4 ms.

over the surface of the eagle's wing. Specifically, because the tips of the upperwing covert feathers point in the direction of the oncoming flow, their aeroelastic deflection indicates a reversed flow. Such flow reversals are in turn indicative of flow separation. Our data reveal two qualitatively different patterns of upperwing covert feather deflection. In the first case, observed during downstrokes in flapping flight (e.g. Fig. 3) and gust response in soaring (e.g. Fig. 4), deflection of the upperwing coverts is largely restricted to the greater coverts, which are the posteriormost row of covert feathers (Fig. 2). In the second case, observed during both gliding and flapping perching sequences, deflection of the upperwing coverts involves all of the different rows of secondary coverts, across practically the entire area that they cover (Fig. 8C, left wing). Whereas the former pattern of deflection indicates that the flow is separated at the trailing edge but attached over the anterior portion of the wing, the latter pattern of deflection indicates that the flow is separated across the entire suction surface of the arm-wing.

In the final stage of a perching manoeuvre, the upperwing coverts are deflected across the entire area they cover, indicating that the flow is stalled over both the arm-wing and the hand-wing. The flow observed during this final deep stall phase of gliding and flapping perching sequences indicates that the wing is operating at a very high angle of attack. In the earlier stages of this deep stall, however, covert feathers distal of the wrist are not deflected, even though the more proximal secondary coverts are completely deflected. This suggests that it is possible for the flow over the hand-wing to generate useful lift even if the flow over the arm-wing is completely stalled. This is consistent with the suggestion that the arm- and hand-wings are able to operate distinctly (Videler, 2005). For example, the hand- and arm-wings of swifts *Apus apus* appear to have distinct aerodynamics during gliding, the arm section experiencing typical fixed-wing attached flow, but with a leading-edge vortex on the hand section (Videler et al., 2004).

The distinct aerodynamics of the arm- and hand-wings of the eagle during the deep stall is not necessarily surprising. We have already said that the wing operates more like a parachute than a conventional wing at this stage of the manoeuvre, and given its spread-eagled posture, the bird may be roughly approximated as a cross parachute (Shen and Cockrell, 1988), with the cross extending wing tip to wing tip and head to tail. The flow characteristics of cross parachutes typically involve relatively high powered jets between the parachute arms (Fig. 9), with the flow near the tips of the canopy arms remaining attached but with separation nearer the crossing point of the arms being encouraged by the jets between them. This is qualitatively similar to the pattern of flow separation and attachment that we observe on the eagle. What is perhaps surprising is that, although the wing is continuously morphing, the flow still exhibits this parachute-like aerodynamic behaviour, even though the shape can only reasonably be approximated during a 20 ms time interval.

Whereas deflections of the upperwing coverts can be used to visualise trailing-edge separation, deflections of the underwing coverts allow us to make inferences about the location of the forward stagnation line. The flow about the wing ahead of the forward stagnation line runs forward around the leading edge, and hence if the stagnation line falls aft of the tips of the underwing coverts, then the feathers will be lifted by air flowing under their tips. Aft movement of the forward stagnation line occurs on any wing as the angle of attack increases (e.g. Barnard and Philpott, 1989). The deflection of the underwing covert feathers that we observe during downstrokes in flapping flight, gust response in soaring, and gliding and flapping perching sequences therefore implies that the lift on the wing is increasing as a result of an increase in the angle of attack. This conclusion is consistent with the trailing-edge separation that is observed during the same manoeuvres.

What sensory information might the covert feathers and alula provide?

So far we have used the covert feathers as a means to visualise the flow around the bird. Although we cannot exclude the possibility that deflection of the covert feathers is merely incidental to the bird, it is possible that the feathers may provide it with similar information to us on the state of the flow, acting as receptors providing continuous aerodynamic feedback during manoeuvres. Nerve recordings from the follicle receptors of the upperwing coverts of chickens *Gallus domesticus* show that the firing rate of the receptors is approximately linear in the angle of elevation of the feather during manual deflection (Brown and Fedde, 1993). The same receptors are also stimulated by passive deflection of the feathers in an airflow as the angle of attack of the wing is increased past the stall point (Brown and Fedde, 1993). Hence, it is reasonable to assume that the eagle has available to it information on the degree and extent of deflection of its covert feathers during flight.

What aerodynamically meaningful feedback might covert feather deflection provide to the bird? The deflection of the upperwing coverts enables us to identify the extent of flow separation across the suction surface of the wing. Specifically, the number of rows of coverts that are deflected indicates the approximate chordwise position of the separation line. It follows that the bird could use the extent of deflection of its upperwing coverts to provide aerodynamic feedback on the degree of stall. Similarly, deflection of the underwing coverts enables us to identify the approximate position of the forward stagnation line, where flow attaches to the wing just beneath the leading edge. It follows that the bird could use the extent of deflection of its underwing coverts to provide aerodynamic feedback on its instantaneous lift coefficient – at least at the high angles of attack at which the underwing coverts are deflected. This kind of information would be especially useful during unsteady manoeuvres in which the instantaneous kinematic state of the wing is insufficient to infer its instantaneous aerodynamic state because of integrated time-history effects (Taylor, 2007).

In addition to the passive deflections of the coverts that we observe, the initial peeling up of the alula from its tip in gliding perching sequences is clearly a passive response to high angle of attack. It is possible that the active protraction of the alula that follows this initial passive deflection is stimulated directly by it, as the alula joint in other species is known to have the necessary receptors for such a response (Brown and Fedde, 1993). Although we have no direct evidence as yet to support this sensory hypothesis, it is attractive in that the alula would then only be deployed at the high angles of attack at which high-

lift devices are useful. High-lift devices have no advantages at low angles of attack, at which they simply add to the total drag on the aerofoil, and an automatic mechanism of this sort would ensure that the alula was only deployed when it was needed. Independent of whether passive deflection of the alula actually stimulates its active protraction, our observation that passive deflection precedes active protraction helps clarify earlier controversy, based on data from wind tunnel experiments with isolated wings, over whether the alula deploys passively or actively (Graham, 1930; Brown, 1963; Nachtigall and Kempf, 1971; Alvarez et al., 2001).

What aerodynamic influence might the covert feathers have?

Deflections of the covert feathers do not merely indicate patterns of flow separation and attachment: since they modify the boundary conditions, they must inevitably affect the flow in some way. This raises the important question of whether these effects are small enough to be considered negligible or whether alternatively they modify the flow sufficiently to have significant aerodynamic consequences for the bird. Analysis of the video data we have collected suggests that if deflections of the covert feathers do indeed have a significant aerodynamic function, then it is complex.

The upperwing coverts rarely deflect as a group, unlike the underwing coverts. Instead they most often deflect individually, or in small local patches. Deflection of the upperwing coverts has the potential to limit the forwards extent of reversed flow, by forcing the separation point to rest at the base of each successive upperwing covert as it lifts (Schatz et al., 2004). Thus they may, in effect, act as a series of ratchet or valve-like features: deflections of single upperwing coverts, or groups thereof, might locally delay separation, which might in turn result in a significant global delay, increasing the effective maximum operating angle of attack of the wing (see Schatz et al., 2004). This is a fundamentally different hypothesis of function from previous suggestions that the upperwing coverts act as turbulators or vortex generators (Blick, 1976). The coverts cannot be acting as turbulators or vortex generators in our eagle, as an attached flow would be needed across the upper surface of the wing for this to be useful. Moreover, the fact that the upperwing coverts deflect from tip to base demonstrates that they are raised by a reversed – and hence already separated – flow.

In contrast to the chaotic deflections of the upperwing coverts, the coherence with which the underwing coverts deploy makes them strongly reminiscent of certain leading-edge flaps used on aircraft during take-off and landing manoeuvres (see Hertel, 1963; Blick, 1976; Azuma, 1992). A flap that protrudes continuously from the leading edge of a wing is known as a Kruger flap, and serves to augment and extend the lift curve slope of a typical high-aspect ratio wing (Hoerner, 1965). Such flaps are used in particular during take-off and landing, which is also when we observe deployment of the underwing coverts in the eagle. The use of leading-edge flaps as high-lift devices on aircraft wings might suggest that the underwing coverts have a similar function in the eagle, although the flexible feathers have a number of properties that set them apart from a conventional rigid flap. Specifically, the leading-edge structure formed by the underwing coverts is (i) passively deployed, (ii) porous and (iii) composed of many discrete elements. What effect might these differences have?

(i) It is clear from the manner in which the underwing coverts are deflected from the tip that the force driving their deployment is aerodynamic, not muscular. This is not to say, however, that the eagle has no direct control over when and whether the coverts are deployed. In support of this, the leading edge flap is consistently used during landings, but not for all landings and not always to the same degree. This might reflect subtle differences in the flow conditions associated with each landing, but might also reflect direct muscular control. For example, by varying the force acting on the feather shaft, it could be possible for the bird to resist passive lifting of the coverts. If the underwing coverts actually have a specific function during manoeuvres, then it would make sense that the eagle would have some form of control over their deployment and retraction.

(ii) All feathers display some degree of porosity, and this does not appear to be significantly greater for the coverts than for the primaries and secondaries (Muller and Patone, 1998). Nevertheless, the transmissivity of the inner vane is typically much lower than that of the outer vane (Muller and Patone, 1998), and it is unlikely that an overlapping row of feathers would allow much air to pass through them. It is unclear how any porosity might affect the operation of a leading-edge flap, but by energizing the boundary layer, any air transmitted through the flap is, if anything, likely to delay separation.

(iii) The leading-edge structure formed by the underwing coverts is composed of a series of discrete overlapping elements, each of which can fully deploy within as little as 8 ms. During manoeuvres, the flap typically either deploys in a wave travelling from the wrist inboard, or in several blocks, broadly corresponding to the shoulder, arm and wrist regions of the wing (Fig. 4). This means that the flap does not behave with the rigidity of a Kruger flap employed on an aircraft, but can instead be partially or fully deployed, potentially allowing a far greater degree of control, whether automatic or modulated. Again this implies a local response to local aerodynamic conditions, which may in itself allow greater resistance to flow separation.

In summary, the various differences between the leading-edge structure formed by the underwing coverts and the leading-edge flaps classically used on aircraft all have the potential to in some way enhance the performance of the structure as a high-lift device. Besides deploying on most landings, the leading-edge structure formed by the underwing coverts was also seen to deploy on every downstroke on which the feathers were visible in flapping flight. The wingbeats we recorded included take-off, mid-flight and landing sequences, and as such the complete consistency with which the structure deployed points to the conclusion that this leading-edge structure deploys every time the bird flaps its wings. This is suggestive of a deliberate and previously unrecognized automatic aeroelastic function for the underwing coverts as a high-lift device in flapping flight.

Wing morphing during gliding perching manoeuvres

The stereotyped gliding and flapping sequences of perching that we have identified both appear to be associated with reducing the eagle's momentum as it comes in to land. In gliding sequences, kinetic energy is exchanged for potential energy as

the bird gains height during the pitch-up phase. Given an estimated groundspeed of 6–9 m s^{-1} and a height gain of approximately 1 m, this could reduce the kinetic energy of landing by some 10–30%. In contrast, the pitch-up phase of flapping perching sequences is not associated with a significant gain of height, and indeed the entire flapping approach is made more or less level with the perch. The eagle's momentum during flapping sequences is therefore reduced not by an interchange of kinetic and potential energy, as in gliding sequences, but only by an aerodynamic mechanism imparting kinetic energy to the wake. Presumably, an interchange of kinetic and potential energy is unnecessary in flapping sequences because sufficient lift for level flight can be generated at lower forward speeds in flapping compared to gliding. Moreover, whereas the aerodynamic deceleration mechanism of flapping perching sequences rests primarily on a single wingbeat with distinct kinematics from those that precede it, the aerodynamic deceleration mechanism used in gliding perching sequences involves a characteristic pattern of wing morphing in which the wing is swept forwards and then back as the bird transitions from gliding flight into a deep stall.

As the wings are flexed during the pitch-up phase of a gliding perching sequence, the hand-wing reaches its maximum sweep and the leading edge of the arm-wing becomes highly curved (Fig. 5D). At this stage, a degree of symmetry is maintained about the wrist section, such that each wing has a delta-shaped planform (Fig. 5, Fig. 6), suggesting that some aspects of delta wing aerodynamics may be paralleled in the eagle's wing at this stage of perching. It is worth noting that the eagle wing has a relatively high radius of curvature at the leading edge, in comparison to a standard delta wing that utilises a sharp leading edge to promote flow separation at low angles of attack (Ericsson and King, 1992). Nevertheless, wind tunnel experiments on delta wings with rounded leading edges suggest that they develop qualitatively similar flows to delta wings with sharp leading-edges at $Re=7\times10^3$ (Miau et al., 1995).

All delta wings generate leading-edge vortices at high angles of attack, beyond the point at which classical high aspect ratio configurations would stall. The adoption of a delta wing planform by each wing may therefore be important in allowing the eagle to generate lift at the high angles of attack necessarily associated with the pitch-up phase of perching leading to the deep stall. The flexion and subsequent protraction of the wing is a highly unsteady motion that is completed in less than 100 ms (Fig. 5), which may be significant because dynamically increasing the angle of sweep of a delta wing is known to increase the angle of attack at which vortex breakdown occurs (Lowson and Riley, 1995). As the wing is straightened and the angle of attack is increased, however, the bursting point of the leading edge vortices is likely to move forwards and the wing will tend towards stall. This may be suppressed on the hand-wing, however, by the active protraction of the alula, which coincides with the point of maximum sweep of the wing. According to this hypothesis, which differs from the classical functional description of the alula as a leading-edge slot or slat (e.g. Nachtigall and Kempf, 1971), the alula would therefore be acting much like a strake on a delta-winged aircraft, serving to promote and stabilise the formation of a leading-edge vortex over the portion of wing behind it (see also Videler, 2005). Hence, while the arm-wing is expected to stall as the wing is protracted at the end of the pitch-up phase, the hand-wing may retain its delta-wing aerodynamics for longer than would be the case without the action of the alula. The protraction of the wings at the end of the pitch-up phase may therefore serve as a transition into the aerodynamics of the deep stall, with the arm-wing becoming fully stalled to act as an aerodynamic decelerator but with the hand-wing still able to generate useful lift.

Besides being the moment of active protraction of the alula, the point of maximum wing flexion is also associated with passive deployment of the underwing coverts. The coverts will only deploy when the stagnation point lies aft of their tips, and this depends upon both the angle of attack of the wing and the length of the feathers. It follows that on an evolutionary timescale, natural selection will be able to determine the specific angle of attack at which the underwing coverts deploy by varying the length of the feathers. Hence, although in an immediate sense the underwing coverts deploy because of the increase in angle of attack associated with the pitch-up phase, in an evolutionary sense the phasing of their deployment with the time of maximum sweep may not be coincidental. Why then might selection favour the deployment of a leading-edge flap at this phase of perching?

When the left and right wings are flexed into deltas, the overall planform assumes a characteristic M-shape (Fig. 5), a shape that is also assumed during flapping flight (Fig. 6). M-shaped planforms were studied during the early stages of the development of delta wings in aircraft, and have some unusual properties. M-wings have a tendency to exhibit a natural pitch-up instability, and use of leading-edge flaps on the wing inner sections has been shown to alleviate this instability (Wyatt and Ilott, 1961). The similarity between the location of the leading-edge structure formed by the underwing coverts of the eagle, and the placement of the leading-edge flaps tested on M-wing designs, is striking (Fig. 10). In the context of perching, it is possible that the natural pitch instability of an M-wing planform contributes to the initial pitch-up manoeuvre, and is then stabilised by the deployment of the leading-edge flap before the bird enters its final deep stall.

The stereotyped nature of the motions associated with perching strongly suggests that the morphing of the wings is not incidental. This morphing includes active changes of planform,

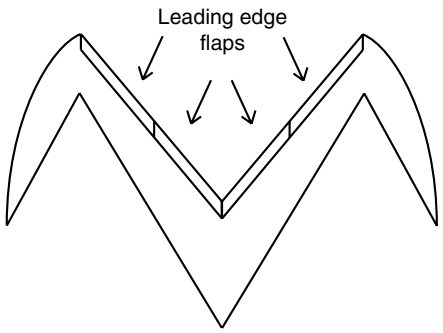

Fig. 10. M-wing planform with adjustable leading edge flaps, used in wind tunnel testing of subsonic and transonic wing designs in the 1960s. (Redrawn from Wyatt and Ilott, 1967.)

passive deflections of coherent structures formed by the coverts, and active but possibly automatic protraction of the alula. Any or all of these features could contribute to the precision and finesse with which a 2.5 kg eagle is able to transition from a flat glide in ground effect to a near-vertical deep stall in less than 0.5 s. Wind tunnel studies are now needed to quantify the aerodynamic effects of these wing morphing and aeroelastic devices.

We thank Louise Crandal and 'Cossack', who first made this work possible, and Martin Cray and Joe Binns for their help during field-testing in Wales. We are grateful to James Gillies and Yukie Ozawa for their contributions to logistical aspects of this research. A.C.C. is a Royal Commission for the Exhibition of 1851 Brunel Research Fellow. G.K.T. is a Royal Society University Research Fellow and RCUK Academic Fellow. Effort sponsored by the Air Force Office of Scientific Research, Air Force Material Command, USAF, under grant number FA8655-05-1-3077. The US Government is authorised to reproduce and distribute reprints for Governmental purpose notwithstanding any copyright notation thereon.

References

Alvarez, J. C., Meseguer, J. and Pérez, A. (2001). On the role of the alula in the steady flight of birds. *Ardeola* **48**, 161-173.

Azuma, A. (1992). *The Biokinetics of Flying and Swimming*. New York: Springer-Verlag.

Barlow, J. B., Rae, W. H. and Pope, A. (1999). *Low-speed Wind Tunnel Testing* (3rd edn). New York: Wiley.

Barnard, R. H. and Philpott, D. R. (1989). *Aircraft Flight: A Description of the Physical Principles of Aircraft Flight* (2nd edn). Harlow: Prentice Hall.

Blick, E. F. (1976). The aerodynamics of birds. *AIAA Stud. J.* **1976**, 4-9.

Brown, R., Ferguson, J. and Lawrence, M. (1987). *Tracks and Signs of the Birds of Britain and Europe: An Identification Guide*. Bromley: Christopher Helm.

Brown, R. E. and Fedde, M. R. (1993). Airflow sensors in the avian wing. *J. Exp. Biol.* **179**, 13-30.

Brown, R. H. J. (1963). The flight of birds. *Biol. Rev.* **38**, 460-489.

Dial, K. P. and Biewener, A. A. (1993). Pectoralis muscle force and power output during different modes of flight in pigeons (*Columba livia*). *J. Exp. Biol.* **176**, 45-55.

Ennos, A. R. and Wootton, R. J. (1989). Functional wing morphology of *Panorpa germanica* (Insecta: Mecoptera). *J. Exp. Biol.* **143**, 275-286.

Ericsson, L. E. and King, H. H. C. (1992). Effect of leading-edge geometry on delta wing unsteady aerodynamics. *J. Aircr.* **30**, 793-795.

Graham, R. R. (1930). Safety devices in the wings of birds. *Br. Birds* **24**, 2-65.

Hertel, H. (1963). *Structure, Form, Movement*. Mainz: Otto Krausskopf-Verlag.

Hoerner, S. F. (1965). Kruger flap. In *Fluid Dynamic Lift*. 2nd edn (ed. H. V. Borst), pp. 6:14-6:15. Bakersfield, CA: Hoerner Fluid Dynamics.

Lowson, M. V. and Riley, A. J. (1995). Vortex breakdown control by delta wing geometry. *J. Aircr.* **32**, 832-838.

Meseguer, J., Franchini, S., Perez-Grande, I. and Sanz, I. L. (2005). On the aerodynamics of leading-edge high-lift devices of avian wings. *Proc. Inst. Mech. Eng. G. J. Aerosp. Eng.* **219**, 63-68.

Miau, J. J., Kuo, K. T., Liu, W. H., Hsieh, S. J., Chou, J. H. and Lin, C. K. (1995). Flow developments above 50-deg sweep delta wings with different leading-edge profiles. *J. Aircr.* **32**, 787-794.

Muller, W. and Patone, G. (1998). Air transmissivity of feathers. *J. Exp. Biol.* **201**, 2591-2599.

Nachtigall, W. and Kempf, B. (1971). Vergleichende Untersuchungen zur Flugbiologischen Function des Daumenfittichs (Alula spuria) bei Vogeln. *Z. Vergl. Physiol.* **71**, 326-341.

Norberg, R. A. (1994). Swallow tail streamer is a mechanical device for self-deflection of tail leading-edge, enhancing aerodynamic efficiency and flight maneuverability. *Proc. R. Soc. Lond. B Biol. Sci.* **257**, 227-233.

Pennycuick, C. J. (1968). A wind-tunnel study of gliding flight in the pigeon *Columba livia*. *J. Exp. Biol.* **49**, 509-526.

Rosen, M., Spedding, G. R. and Hedenstrom, A. (2004). The relationship between wingbeat kinematics and vortex wake of a thrush nightingale. *J. Exp. Biol.* **207**, 4255-4268.

Schatz, M., Knacke, T., Thiele, F., Meyer, R., Hage, W. and Bechert, D. W. (2004). Separation control by self-activated movable flaps. In 42nd AIAA Aerospace Sciences Meeting and Exhibit, Reno, NV, 5-8 January 2004. No. AIAA-2004-1243, www.aiaa.org.

Shen, C. Q. and Cockrell, D. J. (1988). Aerodynamic characteristics and flow round cross parachutes in steady motion. *J. Aircr.* **25**, 317-323.

Stinton, D. (2001). *The Design of the Aeroplane* (2nd edn). Oxford: Blackwell.

Taylor, G. K. (2007). Modelling the effects of unsteady flow phenomena on flapping flight dynamics – stability and control. In *Flow Phenomena in Nature: A Challenge to Engineering Design*. Vol. 1 (ed. R. Liebe), pp. 155-166. Southampton: WIT Press.

Thwaites, B. (1960). Non-planar lifting systems. Ground interference. In *Incompressible Aerodynamics* (ed. B. Thwaites), pp. 527-530. New York: Dover.

Tobalske, B. W. and Dial, K. P. (1994). Neuromuscular control and kinematics of intermittent flight in budgerigars (*Melopsittacus undulatus*). *J. Exp. Biol.* **187**, 1-21.

Videler, J. J. (2005). *Avian Flight*. Oxford: Oxford University Press.

Videler, J. J., Stamhuis, E. J. and Povel, G. D. E. (2004). Leading-edge vortex lifts swifts. *Science* **306**, 1960-1962.

Withers, P. C. (1981). The aerodynamic performance of the wing in red-shouldered hawk *Buteo linearis* and a possible aeroelastic role of wing-tip slots. *Ibis* **123**, 237-248.

Wootton, R. J. (1981). Support and deformability in insect wings. *J. Zool. Lond.* **193**, 459-470.

Wootton, R. J. (1993). Leading edge section and asymmetric twisting in the wings of flying butterflies (Insecta, Papilionoidea). *J. Exp. Biol.* **180**, 117-119.

Wootton, R. J., Kukalová-Peck, J., Newman, D. J. S. and Muzón, J. (1998). Smart engineering in the mid-Carboniferous: how well could Palaeozoic dragonflies fly? *Science* **282**, 753-761.

Wootton, R. J., Evans, K. E., Herbert, R. and Smith, C. W. (2000). The hind wing of a desert locust (*Schistocerca gregaria* Forsk). I. Functional morphology and mode of operation. *J. Exp. Biol.* **203**, 2945-2955.

Wyatt, L. A. and Ilott, G. P. (1961). *Low-speed Pressure-plotting Tests on a Flat-plate M-wing Fitted with Part-span Nose-Flaps* (*ARC-CP-577*). London: Aeronautical Research Council.